Raman scattering study of $RuSr_2R_{2-x}Ce_xCu_2O_{10+\delta}$ (R=Gd,Eu)

A. Fainstein*,† and R. G. Pregliasco†
Centro Atómico Bariloche and Instituto Balseiro, Comisión Nacional de Energía Atómica, 8400 S. C. de Bariloche, Río Negro, Argentina

G. V. M. Williams
Industrial Research Ltd., P.O. Box 31310, Lower Hutt, New Zealand

H. J. Trodahl
School of Chemical and Physical Sciences, Victoria University of Wellington, P. O. Box 600, Wellington, New Zealand
(Received 20 August 2001; revised manuscript received 5 November 2001; published 2 May 2002)

We report a detailed Raman scattering study of polycrystalline samples of the magnetic superconducting ruthenocuprate $RuSr_2R_{2-x}Ce_xCu_2O_{10+\delta}$ (R=Gd,Eu). Samples with varying Ce content (x=0.5,0.7,1.0) and with isotopically substituted ^{18}O have been studied. The assignment of the peaks is analyzed by comparison with the structurally related $RuSr_2RCu_2O_8$ and $Gd_{2-x}Ce_xCuO_4$ oxides. Additional phonon peaks not expected for the reported $I4/mmm$ $RuSr_2R_{2-x}Ce_xCu_2O_{10+\delta}$ space group are observed and are assigned to vibrations rendered Raman active by a symmetry reduction involving rotations of the RuO_6 octahedra. In addition, for x=1 we observe several well defined spin-ordering-dependent features. As a function of decreasing temperature a diffusivelike contribution disappears and below the magnetic ordering temperature (T_M) an underdamped low-energy peak develops and shifts up to $\sim$130 cm^{-1}. A phonon line observed at $\sim$260 cm^{-1} hardens, narrows, and strengthens strongly below T_M. Finally, a phonon line appears below T_M close to the O(Sr) A_{1g} peak. All these features, which are also observed for $RuSr_2RCu_2O_8$, interestingly do not appear for x=0.5. These results point into a structural distortion accompanying the magnetic order, and suggest a complex interplay of spin and lattice degrees of freedom in these ruthenocuprates.

DOI: 10.1103/PhysRevB.65.184517 PACS number(s): 78.30.−j, 74.72.Jt, 74.25.Ha

I. MOTIVATION

The ruthenocuprates $RuSr_2RCu_2O_8$ and $RuSr_2R_{2-x}Ce_xCu_2O_{10+\delta}$ (here R is a rare earth, typically Gd or Eu) have recently attracted strong interest because of the coexistence of high-temperature superconductivity ($T_c \sim 45$ K) with ferromagnetism ($T_M \sim 140$ K).[1,2] In fact, these compounds belong to a larger family of highly correlated oxides, which includes the ruthenates and the manganites, and which display a rich variety of intriguing physical phenomena.[3,4] In particular, for the manganites it is well established that a subtle competition between antiferromagnetic and ferromagnetic order exists, together with a complex interplay of spin, charge, and orbital degrees of freedom.

The information gained recently on the ruthenocuprates also points into a high complexity with many basic questions concerning the magnetic and structural properties remaining unanswered. Magnetic measurements reflect a small remanent magnetization ($\sim 0.1\mu_B$) but a large saturation ($H > 2$ T) magnetic Ru moment $\mu_0(\mathrm{Ru}) \sim 1\mu_B$.[5,6] This result is in apparent contradiction with neutron powder-diffraction measurements performed on $RuSr_2RCu_2O_8$ (RuR_{1212}) which seem consistent with a G-type antiferromagnetic structure in which the Ru moments are antiparallel in all three crystalographic directions.[7,8] In addition, a positive Curie temperature *lower than* T_M has been derived from high-temperature susceptibility measurements,[5] suggesting prevailing ferromagnetic correlations but also some kind of frustration or competition with antiferromagnetism. Interestingly, it has been recently reported from magnetic,[5] x-ray absorption near-edge structure,[9] and nuclear magnetic resonance measurements[10] that Ru in $RuSr_2RCu_2O_8$ exists with mixed Ru^{4+} and Ru^{5+} valence. These valencies correspond to $4d$ electrons with the same electronic configuration of the $3d$ electrons in Mn^{3+} and Mn^{4+}, suggesting the possible existence of competing superexchange and double exchange interactions, and possibly antiferromagnetic-ferromagnetic phase separation.[11,12]

The crystal structure of $RuGd_{1212}$ has been studied both by room-temperature high-resolution transmission electron microscopy[13] and, as a function of temperature, by neutron powder diffraction.[14] In this compound RuO_6 octahedra, which replace the CuO chains in a $RBa_2Cu_3O_7$-type structure, are rotated by about 14° around the c axis. This RuO_6 is partially ordered forming competing domains that differ in the sense of rotation. Within the resolution of the neutron powder diffraction experiments, however, the only structural parameters that seem to respond to the magnetic ordering at T_M are the distance between the two CuO_2 layers and the buckling angle of the CuO_2 planes.[14] This surprising result is also intriguing in view of the Raman scattering data[15–18] reported for RuR_{1212} which display notable changes at T_M, including the appearance of a low-energy peak reminiscent of a structural transition related soft mode.[19]

We report here a Raman scattering study of polycrystalline samples of the related magnetic superconducting ruthenocuprate $RuSr_2R_{2-x}Ce_xCu_2O_{10+\delta}$ [$Ru R(2-x)_{1222}$, R=Gd,Eu]. The structure and physical properties of this compound are similar to those of RuR_{1212}. However, to the best of our knowledge no detailed temperature-dependent structural studies nor Raman experiments have been reported to

date. We have studied samples with varying Ce content ($x=0.5,0.7,1.0$). The assignment of the peaks is analyzed in terms of the reported $I4/mmm$ RuR_{1222} space group and by comparison with the structurally related $RuSr_2RCu_2O_8$ and $Gd_{2-x}Ce_xCuO_4$ oxides. Investigation of isotopically substituted ^{18}O samples are also reported to support these assignments. Magnetic-order-dependent spectral features are observed but only for a certain range of Ce contents. These results are discussed in relation with other ruthenates and the intimate connection between structure and magnetism in these compounds is analyzed.

The paper is organized as follows. In Sec. II we describe the samples and the experimental setup. Section III presents the experimental results which include the temperature, isotope exchange, and Ce content dependencies of the Raman spectra. Finally, in Sec. IV some conclusions are drawn.

II. EXPERIMENTAL

The polycrystalline RuR_{1222} ($R=$Gd,Eu) samples were prepared as described earlier,[6] including a final anneal at 1060 °C in flowing O_2 for seven days. Oxygen isotope exchange was achieved by parallel processing two pieces cut from the same ceramic pellet. Samples were evacuated and then charged with ^{18}O at room temperature, and later annealed in 1 atm at 700 °C. The process was repeated three times to optimize the ^{18}O exchange. A small fraction of Sr_2GdRuO_6 was detected from room temperature x-ray diffraction measurements for Ce content $x\leqslant 0.8$. In addition, extra weak peaks could not be indexed to the $RuSr_2R_{2-x}Ce_xCu_2O_{10+\delta}$ $I4/mmm$ space group or other possible impurity phases for this same Ce content range. The RuO_6 octahedra in $RuSr_2RCu_2O_8$ are known to be rotated about the c axis. Although a similar distortion should be expected in $RuSr_2R_{2-x}Ce_xCu_2O_{10+\delta}$ to accomodate the RuO bonds, this has not been experimentally established yet.[6] The *undistorted* reported $RuSr_2R_{2-x}Ce_xCu_2O_{10+\delta}$ $I4/mmm$ space group structure is shown in Fig. 1. It is essentially a CuO_2 bilayer superconductor as $RuSr_2RCu_2O_8$ but, instead of simply a rare-earth R layer, it contains a $R_{2-x}Ce_xO_2$ block between the CuO_2 layers. This intercalated structure is similar to that seen in the $R_{2-x}Ce_xCuO_4$ so-called T' structure.[20]

Samples with $x=0.5$ and $x=0.7$ are superconducting with T_c in the range 40–50 K, while for $x=1.0$ a semiconductorlike behavior is observed down to 4 K. The magnetic transition temperature, as derived from the onset of an ordered magnetic moment under a small applied magnetic field, decreases from ~ 140 K for $x=1.0$ to ~ 110 K for $x=0.5$.[6]

Raman measurements were performed on a triple subtractive Jobin-Yvon T64000 monochromator coupled to a liquid-N_2 cooled charge coupled device. The 514.5 nm line of an argon ion laser focussed onto a ~ 100 μm diameter circular spot was used for excitation, and the power was kept below 10 mW to minimize the temperature rise at the illuminated spot. The samples were mounted in a continuous flow He cryostat allowing experiments in the 2.5–300 K temperature range.

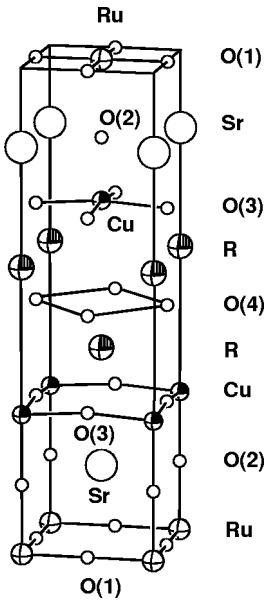

FIG. 1. Structure of $RuSr_2R_2Cu_2O_{10+\delta}$ with space group $I4/mmm$. Only half unit cell is shown. From bottom to top it consists of RuO_2, SrO_2, and CuO_2 layers similar to $RuSr_2RCu_2O_8$. After these planes, instead of simply a rare-earth R layer as in this latter compound, it contains a $R_{2-x}Ce_xO_2$ block separating the two CuO_2 layers. This intercalated structure is similar to that seen in the $R_{2-x}Ce_xCuO_4$ so-called T' structure. Note that consequently the second CuO_2 plane, and on top the SrO_2 and RuO_2 layers, are shifted $(1/2,1/2,z)$ with respect to the bottom part of the cell.

III. RESULTS AND DISCUSSION

A. Phonon Raman spectra and isotope shift

In Fig. 2 (top) we show the Raman spectra collected both at 5 and 240 K for $RuGd1.0_{1222}$ (top and bottom spectrum, respectively). We will concentrate here on those Raman features that do not depend on the magnetic order, leaving the temperature dependencies for the next section. Phonon Raman lines are observed at ~ 103, 136, 156, 218, 253, 326, 385, 402, 443, 485, and 653 cm^{-1}. We only indicate features that, though weak, are systematically observed in an extensive collection of spectra taken from different spots and temperatures. In Table I we give the atomic site symmetry and the irreducible representations for RuR_{1222} with the undistorted $I4/mmm$ structure.[21] In this structure one expects in total 14 $(5A_{1g}+2B_{1g}+7E_g)$ Raman allowed modes. Note that for this structure the ''basal plane'' Ru and O(1) atoms occupy inversion symmetry sites and thus do not participate in Raman active modes. When the possible RuO_6 rotation and tilting as in RuR_{1212} is considered the structure remains with $I4/mmm$ space group but O(1) and O(2), belonging, respectively, to the RuO_2 and SrO_2 layers, change their site symmetry. The corresponding irreducible representations are presented in Table II. In total 14 $(2A_{1g}++2A_{2g}+3B_{1g}+3B_{2g}+4E_g)$ new Raman active modes are added by the distortion. In addition to the duplication of possible Raman modes, the most interesting consequence of the distortion is the activation of O(Ru) vibrations. This is similar to RuR_{1212} for which, in fact, phonons rendered Raman active by the

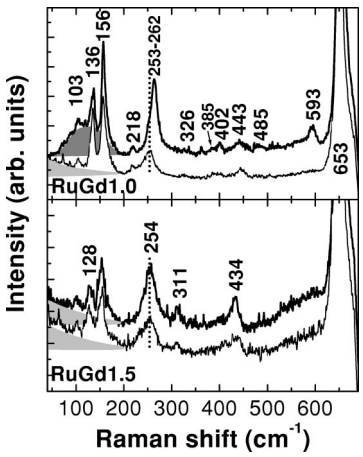

FIG. 2. Top: Raman spectra of polycrystalline $RuSr_2GdCeCu_2O_{10+\delta}$ taken at 240 K (thinner bottom curve) and at 5 K (thicker top curve). The numbers indicate the spectral position of the Raman peaks. The shaded light-grey region shows the diffusivelike scattering observed above T_M. The broad peak that appears below T_M is highlighted with dark-grey shading. Note the strong shift of the ~ 253 cm^{-1} line and the appearance of a new peak at ~ 593 cm^{-1} at low temperatures. Bottom: Raman spectra of polycrystalline $RuSr_2Gd_{1.5}Ce_{0.5}Cu_2O_{10+\delta}$ taken at 240 K (bottom curve) and at 5 K (top curve). The numbers label those peaks that depend most on Ce content. Note that for this sample the diffusivelike scattering remains as an overdamped peak even at low temperatures. In addition, the position of the ~ 254 cm^{-1} peak does not vary with temperature and no new peak appears around ~ 590 cm^{-1}.

RuO_6 rotations and involving these atoms have been reported.[15–18] In view of the many possible Raman active modes and in order to analyze the spectra we consider the following approach. First, we expect that the most intense modes correspond to those already active for the undistorted structure. Secondly, for these modes and similarly to the case of the structurally related high-T_c superconductor $RBa_2Cu_3O_7$, it is plausible to expect that the E_g lines are weak and thus most of the observed lines should correspond to A_{1g} and B_{1g} symmetry vibrations. Thirdly, we assign the observed vibrations by comparison with the spectra of the structurally similar $RuSr_2RCu_2O_8$ and $R_{2-x}Ce_xCuO_4$ compounds. Last, other observed peaks are interpreted as due to the distortion induced symmetry reduction. Note again that the reported $RuSr_2RCu_2O_8$ spectra already include modes activated by the RuO_6 rotations.

TABLE I. Wyckoff notations, atomic site symmetries, and irreducible representations in $RuSr_2R_2Cu_2O_{10+\delta}$ with space group $I4/mmm$, without the RuO_6 octahedra rotation included. O(1) belongs to the RuO_2 planes, O(2) to the SrO_2 layers, O(3) to the CuO_2 planes, and O(4) to the $R_{2-x}Ce_xCuO_4$ block.

Atom	Wyckoff notation	Site symmetry	Irreducible respresentations
Ru	2(a)	D_{4h}	$A_{2u}+E_u$
O(1)	4(c)	D_{2h}	$A_{2u}+B_{2u}+2E_u$
O(2)	4(e)	C_{4v}	$A_{1g}+E_g+A_{2u}+E_u$
O(3)	8(g)	C_{2v}^v	$A_{1g}+B_{1g}+2E_g+A_{2u}+B_{2u}+2E_u$
O(4)	4(d)	D_{2d}	$B_{1g}+E_g+A_{2u}+E_u$
R	4(e)	C_{4v}	$A_{1g}+E_g+A_{2u}+E_u$
Sr	4(e)	C_{4v}	$A_{1g}+E_g+A_{2u}+E_u$
Cu	4(e)	C_{4v}	$A_{1g}+E_g+A_{2u}+E_u$

TABLE II. Wyckoff notations, atomic site symmetries, and irreducible representations in $RuSr_2R_2Cu_2O_{10+\delta}$ with space group $I4/mmm$ including the RuO_6 octahedra rotation. Only the atoms that change their site symmetry due to the distortion are included. The notation is the same as in Fig. 1 and Table I.

Atom	Wyckoff notation	Site symmetry	Irreducible respresentations
O(1)	8(j)	C_{2v}	$A_{1g}+A_{2g}+B_{1g}+B_{2g}+E_g+A_{2u}+B_{2u}+2E_u$
O(2)	16(n)	C_s^v	$2A_{1g}+A_{2g}+2B_{1g}+B_{2g}+3E_g+A_{1u}+2A_{2u}+B_{1u}+2B_{2u}+3E_u$

The measured peak frequencies are given in Table III together with the proposed assignments and phonon group representations. As follows from Table III, all the peaks expected from a comparison with the Raman spectra of the related oxides $RuSr_2RCu_2O_8$ and $R_{2-x}Ce_xCuO_4$ are observed, albeit some of them with notably weak intensity. From this comparison we propose that the ~ 136 cm^{-1} peak is the A_{1g} Cu vibration and the ~ 150 cm^{-1} line corresponds to the A_{1g} Sr mode (these two modes are not resolved in RuR_{1212}). The ~ 326 and ~ 443 cm^{-1} peaks, on the other hand, are the B_{1g} out-of-phase and A_{1g} in-phase O(Cu) vibrations, while the ~ 653 cm^{-1} line is the A_{1g} O(Sr) phonon. All these modes correspond to z-polarized vibrations and have their counterpart in the high-T_c cuprate $RBa_2Cu_3O_7$. On the other hand we assign, in correspondence with RuR_{1212}, the ~ 260 cm^{-1} peak to an A_{1g} O(Ru) vibration. The symmetry of this mode has been derived from polarization resolved measurements in oriented thin films.[17] We recall that this mode is allowed in RuR_{1212} and RuR_{1222} only when the symmetry reduction due to rotations of the RuO_6 octahedra is taken into account. We note that the strongest line observed for $\lambda = 514.5$ nm excitation is the O(Sr) z-polarized vibration in accordance with previous results on $RBa_2Cu_3O_7$ and RuR_{1212}. In contrast, however, the B_{1g} O(Cu) is strong in these later compounds but is almost unobservable in RuR_{1222}.

In addition to the above discussed lines, three modes are observed that can be assigned to the $R_{2-x}Ce_xO_2$ block, namely, the ~ 218 cm^{-1} line corresponding to the A_{1g} rare-earth mode (forbidden both in $RBa_2Cu_3O_7$ and in RuR_{1212}), the ~ 385 cm^{-1} mode probably due to the B_{1g} O(4) vibration and, last, the ~ 485 cm^{-1} line due to the E_g O(4) phonon. The corresponding modes in $Gd_{2-x}Ce_xO_2$ appear at ~ 220, ~ 347, and ~ 492 cm^{-1}, respectively.[20]

In order to verify the above assignments we have performed Raman scattering experiments in ^{18}O exchanged Ru$R1.0_{1222}$ samples for both R=Gd and Eu. These results

TABLE III. RuGd1222 Raman line assignments and isotope shift. The first line gives the line assignment. ZF refers to a ''zone-folding'' peak. NA labels a weak ''not assigned'' peak. The second and third lines correspond to the measured and assigned Raman peaks of $RuSr_2GdCu_2O_8$ (from Ref. 14) and $Gd_{1.85}Ce_{0.15}CuO_4$ (taken from Ref. 19). The fourth line corresponds to the $RuSr_2Gd_{1.0}Ce_{1.0}Cu_2O_{10+\delta}$ peak positions reported here. The last line gives the isotope shift for ^{18}O substitution as compared to that expected from the $\sqrt{m(^{16}O)/m(^{18}O)}$ ''mass rule'' (in percent shift). Due to its weak intensity we have not been able to determine precisely the isotope shift of the B_{1g}[O(Cu)] mode.

Peak	NA	A_{1g}(Cu)	A_{1g}(Sr)	A_{1g}(Gd)	A_{1g} [O(Ru)]	B_{1g} [O(Cu)]	B_{1g} [O(4)]	ZF	A_{1g} [O(Cu)]	E_g [O(4)]	ZF	A_{1g} [O(Sr)]
RuGd1212	107		150		250-260	310		412	420		605	650
GdCe214				220			347			492		
RuGd1222	103	136	156	218	253–262	326	385	402	443	485	593	653
Isoshift (%)	NO	NO	40	NO	75		100	100	80	90	97	95

are shown in Fig. 3 for $T=2.5$ K. The measured isotope shifts are given in Table III. These shifts are given as the ratio between the measured shift and that expected from the $\sqrt{m(^{16}O)/m(^{18}O)}$ ''mass rule'' considering complete oxygen exchange. We found that all Raman modes above ~ 350 cm^{-1} shift, within experimental error, consistently with an almost 100% exchange. The O(Cu) A_{1g} mode, on the other hand, displays a somewhat reduced shift of about 80%. This can be understood as due to a non complete oxygen exchange at the O(Cu) site, an observation consistent with the fact that the CuO_2-plane oxygen atoms are the most difficult to exchange in the related $RBa_2Cu_3O_7$ compounds.[22] We also observe a reduced 75% shift for the phonon line assigned to O(Ru) in the RuO_2 planes. This result suggests that O(Ru) is also relatively difficult to exchange, although this would contrast with $RBa_2Cu_3O_7$ where the O(1) chain oxygens are relatively easy to remove. In any case, it is quite clear that all phonons above ~ 250 cm^{-1} correspond to vibrations involving mainly oxygen displacements. Conversely, the A_{1g} Cu ~ 136 cm^{-1} and A_{1g} Gd ~ 218 cm^{-1} lines do not display, as expected, any dependence with ^{18}O exchange. What is somewhat surprising, however, is the well defined 40% shift observed for the ~ 150 cm^{-1} line we assigned to the A_{1g} Sr phonon. We note that a similar oxygen isotope shift is not observed for the corresponding mode in $RBa_2Cu_3O_7$. We speculate that the A_{1g} Sr phonon couples to the A_{1g} O(Ru) mode at ~ 253 cm^{-1}. This assumption is supported in that the latter mode is close in energy to the A_{1g} Sr phonon, and involves atoms [O(Ru) and probably O(Sr)] located close to Sr in the RuR_{1222} structure. Such mode coupling also provides, on the other hand, an alternative and consistent explanation for the relatively small 75% isotope shift of the A_{1g} O(Ru) vibration discussed above.

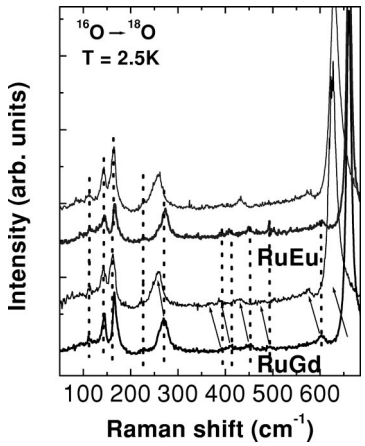

FIG. 3. Polarized Raman spectra of polycrystalline $RuSr_2RCeCu_2O_{10+\delta}$ taken at 5 K for $R=$Gd and Eu and for both oxygen isotopes ^{16}O and ^{18}O. The two top curves correspond to $R=$Eu, the other two to Gd. For each pair, the top curve is the ^{18}O exchanged sample. The arrows highlight the peaks that shift denoting their oxygen character. See Table II for the peak positions and isotope shift of each Raman peak.

Before finishing this section, we note that two other weak peaks are seen for RuR_{1222} at ~ 103 and ~ 402 cm^{-1}, which have their counterpart in RuR_{1212}. The ~ 402 cm^{-1} mode displays complete ^{18}O isotope shift, while the ~ 103 cm^{-1} line clearly involves no oxygen displacement. In Ref. 16 the ~ 402 cm^{-1} peak has been assigned to a folded phonon rendered active by the doubling of the unit cell produced by the rotations of the RuO_6 octahedra, thus also supporting a similar symmetry reduction in RuR_{1222}. The ~ 103 cm^{-1} line, on the other hand, remains to be assigned.

B. Temperature dependence

In addition to the phonon lines described above, several distinctive strongly temperature dependent features can be discerned for RuGd1.0$_{1222}$ in Fig. 2 (top). Namely, (i) a low-energy diffusive contribution (indicated with light gray shading in the 240 K spectrum), (ii) a well defined broad peak centered around ~ 130 cm^{-1} and observable only at low temperatures (indicated with darker gray shading in the 5 K spectrum), (iii) the shift, narrowing, and enhancement of the A_{1g} O(Ru) line with decresing temperature, and (iv) the abrupt appearance of a new line at low temperature at ~ 593 cm^{-1}. Note that, above T_M, only a broad and weak structure persists on the leading edge of the 653 cm^{-1} peak. In order to avoid any indetermination in correcting by the Bose factor, we show in Fig. 2 and hereafter the raw data. Thus, the low-energy features described in (i) and (ii) have not been corrected by this factor. We note, however, that this correction only produces minor changes at 240 K and no effect at all at 5 K.

In Fig. 4 we show the temperature dependence of the RuGd1.0$_{1222}$ spectra taken from room temperature down to 5 K. It is clear from this figure that the shift of the A_{1g} O(Ru)

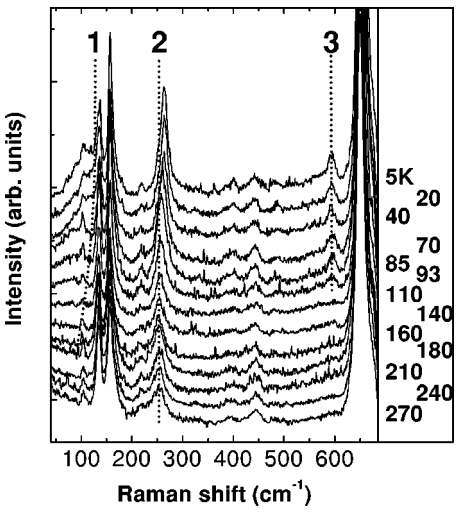

FIG. 4. $RuSr_2GdCeCu_2O_{10+\delta}$ spectra taken at various temperatures (nominal) above and below $T_M \sim 140$ K. Note the spin-order-dependent features: the diffusive low-energy component observed at high temperatures, the ~ 130 cm^{-1} peak that develops below T_M (1), the hardening of the ~ 253 cm^{-1} phonon line assigned to O(Ru) vibrations (2), and the abrupt appearance of a peak at ~ 593 cm^{-1} below T_M (3).

line, and the appearance of the ~ 130 and ~ 593 cm^{-1} peaks, develop together below the magnetic ordering temperature T_M. On the other hand, the diffusive contribution dissapears with decreasing temperature. We note that similar features have been observed previously for RuGd1212.[15–17] We have observed from a detailed study in RuGd1212 sintered samples that the diffusive contribution displays, in addition to the usual Bose-factor temperature dependence, an abrupt decrease at T_M.[23] In addition, we found[17] a kind of sum rule that connects the intensity of the ~ 130 cm^{-1} peak and the diffusive scattering, pointing into a common origin for the two features. As we will show below, the $RuGd_{1222}$ sample with $x=0.5$ shows no peak at ~ 130 cm^{-1}, but it retains the diffusive tail to low temperature giving further support to the suggestion that the two contributions are related. Two scenarios have been proposed to account for the appearance of the low-energy ~ 130 cm^{-1} peak below T_M, namely, magnetic excitations[15,16] and a vibrational mode activated by a magnetostriction induced structural distortion.[17] Within the latter description the diffusive contribution is understood as due to overdamped excitations that becomes underdamped below T_M leading to the ~ 130 cm^{-1} peak. The picture is similar to the soft-phonon features observed for KDP and described in Ref. 19.

The ~ 593 cm^{-1} line, on the other hand, displays almost 100% oxygen isotope shift evidencing its oxygen phonon character. We believe it is a O(Sr) band folded phonon rendered active by the doubling of the unit cell produced by the rotations of the RuO_6 octahedra.[16] An increase of intensity with decreasing temperature of this line and the other zone-folded peak at ~ 402 cm^{-1} has been also reported for $Ru R_{1222}$.[16] This behavior has been proposed in Ref. 16 to be an indication of spin dependent phonon Raman scattering as introduced by Suzuki and Kamimura.[24] We note, however, that the abrupt appearance below T_M of the ~ 593 cm^{-1} line displayed in Fig. 4 can also be interpreted as an indication that some kind of structural transition related with the rotation of the RuO_6 octahedra sets in together with the three dimensional magnetic order. This interpretation would be consistent with the phonon description of the ~ 130 cm^{-1} peak discussed above. As we will show in the next section, the Ce content dependence of the Raman spectra in $Ru R_{1222}$ provides new insight into the physical origin of the observed features.

C. Ce-content dependence

We have performed Raman scattering studies of $Ru R_{1222}$ with $R=$Gd and Eu, and with Ce contents $x=0.5$, 0.7, and 1.0. For both rare earths the same conclusions apply, the only difference being that the observed magnetic order dependent features are systematically weaker for $R=$Eu.[16] The most relevant results concerning the Ce-content dependence are displayed in Fig. 2 (bottom), where we show Raman spectra taken both at 5 and 240 K for $RuGd_{1222}$ with $x=0.5$. These spectra should be compared with those for $x=1.0$ shown in the top part of the same figure. In addition to the poorer signal to noise ratio, reflected in the identification of fewer lines, the most relevant observations are as follows. (i) For $x=0.5$ none of the magnetic-order-dependent features appear. In fact, the low-energy diffusive contribution remains as an overdamped signal and no feature reminiscent of the low-energy ~ 130 cm^{-1} line is observed down to the lowest temperature. In addition, the ~ 254 cm^{-1} phonon line assigned to an O(Ru) vibration does not shift with decreasing temperature and, finally, no discernible phonon peak develops around ~ 590 cm^{-1}. Note that for $x=0.5$ a broad structure is observed in the range $\sim 500-600$ cm^{-1}. This feature does not display any notable change at T_M, and we believe that it could be due to the small fraction of Sr_2GdRuO_6 present in this sample. We recall that $T_M \sim 110$ K for $Ru R1.5_{1222}$, well above our lowest attainable temperature. In addition, the magnetic properties are qualitatively similar for the samples with different Ce content.[6] (ii) The three peaks that depend most on the Ce content [labeled with their Raman shift in Fig. 2 (bottom)] are the A_{1g} Cu, the B_{1g} O(Cu), and the A_{1g} O(Cu) phonon lines. All these modes involve atoms belonging to the CuO_2 planes. We note that the atomic radii of Gd^{3+} and Eu^{3+} are similar (1.053 and 1.066 Å, respectively), while that of Ce^{4+} is much smaller (~ 0.9 Å). This implies that the CuO_2 bilayer separation should decrease for higher Ce contents, in agreement with the observed hardening of the CuO_2 related phonons. (iii), The A_{1g} O(Ru) Raman mode is observed also for $x=0.5$ implying that the RuO_6 octahedra rotations are present for the full range of studied Ce contents. We note that for $x=0.7$ we have observed the same magnetic order dependent features as for $x=1$ though with a much reduced intensity. The spectra denote a continuous evolution from $x=1$ to $x=0.5$ for the three studied compositions.

Point (i) above is, on one hand, definitive evidence that the three magnetic-order-dependent features have a common origin. On the other hand, since the atomic replacement of

Gd by Ce does not significantly alter the magnetic properties, it strongly indicates that the observed phenomena reflects a structural effect rather than a coupling to magnetic excitations. In fact, the A_{1g} O(Ru) line shift, the abrupt appearance of the ~ 593 cm^{-1} phonon, and the development of the low-energy peak below T_M, all together suggest that the onset of magnetic order is accompanied by structural changes involving the RuO_6 octahedra. The detailed atomic displacements associated with the transition are not yet clear, nor is the origin of the low-energy excitations responsible for the broad feature at 130 cm^{-1} in the magnetic phase. To date there are no temperature-dependent x-ray or electron diffration studies for these materials, so that one can only speculate about these issues. We suggest that the effects of magnetostriction serve to restrict reorientation of the RuO_6 octahedra, possibly leading to intermediate- or long-range order in their rotational sense. Within this scenario the low-energy excitations can be understood as an overdamped vibrational mode involving the O(Ru) ions, which then hardens and becomes underdamped below T_M. The strong shift, narrowing and enhancement of the A_{1g} O(Ru) peak below T_M could evidence, within this picture, the coupling with the A_{1g} 130 cm^{-1} mode of the same symmetry. Such mode coupling in structural transitions and with a similar phenomenology has been described previously, e.g., by Barker and Hopfield[25] and by Hayes and Loudon.[19]

Point (ii) above, on the other hand, implies that the main effect of decreasing the Ce content is to increase the distance between the CuO_2 planes. The related nonobservation of the spin ordering dependent Raman features suggests that this CuO_2-CuO_2 separation is relevant for the structural distortion induced at T_M. This might be unexpected in view of the fact that the CuO_2 planes are structurally separated from the magnetic RuO_2 planes. However, a connection between the CuO_2-CuO_2 plane separation and the magnetic order has also been derived from neutron scattering data.[14] These results show an anomalously large temperature dependence of the CuO_2-CuO_2 separation above T_M (consistent with an expansion coefficient three times larger than that of the c axis), which turns into an almost temperature independence once the magnetic order is established.

IV. CONCLUSIONS

In conclusion, several phonon peaks are observed for $RuSr_2R_{2-x}Ce_xCu_2O_{10+\delta}$ (R=Gd,Eu) and have been assigned by comparison with the structurally related $RuSr_2RCu_2O_8$ and $Gd_{2-x}Ce_xCuO_4$ oxides. Phonon peaks not expected for the reported $I4/mmm$ space group are observed and are explained as due to the doubling of the unit cell produced by rotations of the RuO_6 octahedra. In addition, for $x=1$ we observe well defined spin-order-dependent features. The appearance of a zone-folded Raman peak at T_M, and the nonobservation of these magnetic-order dependent features for $x=0.5$, suggest that a structural transition is induced by the establishment of magnetic order. The microscopic description of the magnetic-order induced structural transition and the precise assignment of an observed low-energy Raman peak remain to be established. We have proposed based on the results reported here that magnetostriction effects freeze or establish a long-range order of the RuO_6 rotations in the RuO_2 planes. Within this scenario the low-energy excitations are understood as vibrational modes which are overdamped above T_M but become underdamped leading to a well defined peak once the magnetic order is established. Temperature-dependent high resolution electron microscopy could probably clarify these issues, and determine whether some kind of charge or orbital ordering accompanies the magnetic transition. Our results suggest a complex interplay of spin and lattice degrees of freedom in these ruthenocuprates.

Note added. We note the publication after submission of this manuscript of a paper reporting Raman scattering data on single crystals of $RuGd_{1212}$.[26] The derived phonon symmetries confirm previous assignments deduced from sintered and film samples.[15–17] These assignments support the identification of the Raman lines of $RuGd_{1222}$ reported here which are based in a comparison with $RuGd_{1212}$. In addition, structural data of RuR_{1222} have been reported which confirms the existence of a symmetry reduction due to RuO_6 octahedra rotations in these compounds.[27]

*Email address: afains@cab.cnea.gov.ar
†Also at CONICET, Argentina.

[1] I. Felner, U. Asaf, Y. Levi, and O. Millo, Phys. Rev. B **55**, R3374 (1997).
[2] C. Bernhard, J. L. Tallon, Ch. Niedermayer, Th. Blausius, A. Golnik, E. Brucher, R. K. Kremer, D. R. Noakes, C. E. Stronach, and E.J. Ansaldo, Phys. Rev. B **59**, 14 099 (1999).
[3] M. Imada, A. Fujimori and Y. Tokura, Rev. Mod. Phys. **70**, 1039 (1998).
[4] Y. Tokura and N. Nagaosa, Science **288**, 462 (2000).
[5] A. Butera, A. Fainstein, E. Winkler, and J. L. Tallon, Phys. Rev. B **63**, 054442 (2001).
[6] G. V. M. Williams and M. Ryan, Phys. Rev. B **64**, 094515 (2001).
[7] J. W. Lynn, B. Keimer, C. Ulrich, C. Bernhard, and J. L. Tallon, Phys. Rev. B **61**, 14 964 (2000).
[8] J. D. Jorgensen, O. Chmaissem, H. Shaked, S. Short, P. W. Klamut, B. Dabrowski, and J. L. Tallon, Phys. Rev. B **63**, 054440 (2001).
[9] R. S. Liu, L.-Y. Jang, H.-H. Hung, and J. L. Tallon (unpublished).
[10] Ken-ichi Kumagai, Satomi Takada, and Yuji Furukawa, Phys. Rev. B **63**, 180509 (2001).
[11] E. Dagotto, T. Hotta, and A. Moreo, Phys. Rep. **344**, 1 (2001).
[12] For a model applied to the ruthenocuprates that introduces competing antiferromagnetic and double exchange ferromagnetic interactions see H. Aliaga and A. A. Aligia, Physica B (to be published).
[13] A. C. McLaughlin, W. Zhou, J. P. Attfield, A. N. Fitch, and J. L. Tallon, Phys. Rev. B **60**, 7512 (1999).
[14] O. Chmaissem, J. D. Jorgensen, H. Shaked, P. Dollar, and J. L. Tallon, Phys. Rev. B **61**, 6401 (2000).
[15] V. G. Hadjiev, A. Fainstein, P. Etchegoin, H. J. Trodahl, C. Bernhard, M. Cardona, and J. L. Tallon, Phys. Status Solidi B **211**, R5 (1999).

[16] A. Fainstein, P. Etchegoin, H. J. Trodahl, and J. L. Tallon, Phys. Rev. B **61**, 15468 (2000).
[17] A. Fainstein, A. E. Pantoja, H. J. Trodahl, J. E. McCrone, J. R. Cooper, G. Gibson, Z. Barber, and J. L. Tallon, Phys. Rev. B **63**, 144505 (2001).
[18] M. N. Iliev, A. P. Litvinchuk, V. N. Popov, R. L. Meng, L. M. Dezaneti, and C. W. Chu, Physica C **341-348**, 2209 (2000). This paper presents Raman phonon mode assignments for RuR_{1212} based on group theory and lattice dynamical calculations.
[19] See, for example, N. Hayes and R. Loudon, *Scattering of Light by Crystals* (Wiley, New York, 1978), p. 112.
[20] E. T. Heyen, R. Liu, M. Cardona, S. Piñol, R. J. Melville, D. McK. Paul, E. Morán, and M. A. Alario-Franco, Phys. Rev. B **43**, 2857 (9191).
[21] D. L. Rousseau, R. P. Bauman, and S. P. S. Porto, J. Raman Spectrosc. **10**, 253 (1981).
[22] V. G. Ivanov, M. N. Iliev, and C. Thomsen, Phys. Rev. B **52**, 13 652 (1995).
[23] A. Fainstein, J. H. Trodahl, and J. L. Tallon (unpublished).
[24] N. Suzuki and H. Kamimura, J. Phys. Soc. Jpn. **35**, 985 (1973).
[25] A. S. Barker, Jr. and J. J. Hopfield, Phys. Rev. **135**, A1732 (1964).
[26] V. G. Hadjiev, J. Bäckström, V. N. Popov, M. N. Iliev, R. L. Meng, Y. Y. Xue, and C. W. Chu, Phys. Rev. B **64**, 134304 (2001).
[27] G. V. M. Williams, A. C. McLaughlin, J. P. Attfield, S. Krämer, and Ho Keun Lee, Phys. Rev. B (to be published).